Critical Dynamics in the Pearling Instability of Membranes

Roy Bar-Ziv,[1] Tsvi Tlusty,[2] and Elisha Moses[1]
[1]*Department of Physics of Complex Systems, The Weizmann Institute of Science, Rehovot 76100, Israel*
[2]*Department of Materials and Interfaces, The Weizmann Institute of Science, Rehovot 76100, Israel*
(Received 17 October 1996)

We report quantitative measurements above threshold in the pearling instability of cylindrical membranes. Induced by optical tweezers, the instability propagates outward from the laser trap with well defined wavelength, and velocity. All measured quantities scale with the reduced tension control parameter $\epsilon \equiv (\Sigma - \Sigma_c)/\Sigma_c$. A critical slowing down for initiation of the instability is observed. The values of the velocity, wavelength, and delay time agree with marginal stability and linear analysis. Measurements very close to threshold are strongly masked by thermal fluctuations. [S0031-9007(97)03733-2]

PACS numbers: 87.22.Bt, 47.20.Dr, 68.10.–m

Dynamical shape transitions of membranes are inherently more complex than their static configurations. The equilibrium shapes can be explained by variants of the Helfrich curvature energy alone [1,2]. The nonlinear dynamics, on the other hand, involve the interaction of the curvature with the flow of the surrounding fluid, with thermal fluctuations, and, as we now understand, with an effective tension as well [3,4]. Demonstrating that nonlinear dynamical methods can be quantitatively accurate in such a system is therefore of some importance.

Recently we reported a novel "pearling" instability in cylindrical fluid membranes induced by application of optical tweezers [5]. The action of the tweezers is to pull lipid material into the trap region, inducing an effective tension in the rest of the membrane. Upon tweezing, membrane tubes develop a Rayleigh-like peristaltic instability with a well defined wavelength, advancing into the thermally fluctuating tube. The origin of the pearling instability has been identified as a competition between the destabilizing external tension Σ induced by the laser and the bending rigidity of the membrane κ [5–8]. Above a critical tension Σ_c a membrane tube becomes unstable to long wavelength peristaltic modes.

The difficulties in obtaining quantitative data from the transition lie first in the experimental control of the instability, and then in the thermal fluctuations which mask its onset. The first problem was solved by using the laser tweezers [9] to controllably and gradually increase the control parameter until onset was reached. The second problem is deeper, since it essentially rules out measurements of the linear state, and without such information predicting or measuring nonlinear coefficients and behavior is impractical.

We therefore exploited the fact that the instability propagates outward from the tweezing point, with a leading edge that exhibits well defined velocity and wavelength selection [5,10]. Work on dynamical systems has shown that the propagating solution often obeys a criterion of marginal stability (MSC) [11]. The front is then determined not by the high amplitude, nonlinear state behind the front, but by the linear properties of this low amplitude leading edge.

Our major results are as follows.

(1) We measure a constant velocity of propagation of the unstable pearling front that depends linearly on the control parameter $\epsilon \equiv (\Sigma - \Sigma_c)/\Sigma_c$. This is in agreement with the MSC analysis of Goldstein, Nelson, Powers, and Seifert (GNPS) [10].

(2) Critical slowing down is observed, with a delay time for initiation of the pearling that scales like ϵ^{γ} with $\gamma = -1.0 \pm 0.15$. We propose an explanation of this in terms of a linear response calculation.

(3) The selected wave vectors lie on a curve that rises from below 0.5 (in units of the tube radius) at low ϵ to about 1.0 at high ϵ, in better agreement with predictions of the MSC [10] than with the fastest growing mode from linear theory [6].

(4) Long wavelength, small amplitude propagating waves that are barely discernible immediately at onset are suppressed and replaced by larger amplitude, nonlinear states with shorter wavelength.

(5) The estimate of laser induced tension from electrodynamic considerations is confirmed by the measured threshold intensity at onset of the instability.

(6) The agreement between the experiment and the linear calculations extends up to $\epsilon \approx 20$. Close to threshold, $\epsilon \leq 1$, the instability is indeed masked by thermal fluctuations of the membrane.

Experiment.—The quantitative measurements presented here were performed on tubes of stearoyl-oleoyl-phosphatidylcholine (SOPC, Sigma) lipids in water with 0.5 M glucose at room temperature. Unilamellar tubes, freely suspended between large lipid globules were produced as reported previously [5]. Tubes were hundreds of μm long and with radii in the range $R_0 \approx 0.4$–1.0 μm. The optical tweezers setup is by now standard [12], except for the use of an Ar laser. Laser power intensities ranged from 6 to 50 mW. The laser was turned on for a duration long enough to observe pearling but short enough to prevent the tube from going into the highly nonlinear

 0031-9007/97/79(6)/1158(4)$10.00

regime. That state is quite different, characterized by isolated tense pearls that propagate along the thinned out tube [5,13]. Our procedure also allows rapid relaxation of the membrane to a straight tube with little remnant effect on the tube. Theoretically, the laser induced tension is given by $\Sigma_L = I\Delta\bar{\epsilon}D/c\omega_0^2$ [6] where I is the laser power in the trap, $\Delta\bar{\epsilon} \approx 0.23$ is the dielectric difference of lipids and water in the visible range, $D \approx 40$ Å is the membrane thickness, c is the speed of light in water, and $\omega_0 \approx 0.3$ μm is the size of the trap. Similarly, the critical tension for pearling is $\Sigma_c = \frac{3}{2}\kappa/R_0^2$ [5], where κ is the bending rigidity of the membrane ($\approx 10^{-12}$ erg for SOPC [4]).

Experimentally, the onset of pearling occurred when the laser intensity exceeded a critical intensity I_c which we measured to be $I_c = 10 \pm 4$ mW on tubes of radius $R_0 = (0.6 \pm 0.1)$ μm. Using these values we obtain $\Sigma_L = 4.5 \times 10^{-4}$ erg/cm^2 and $\Sigma_c = 4.2 \times 10^{-4}$ erg/cm^2 with errors of up to 40% in both. The agreement between the two estimates of the tension is a confirmation of the simple electrodynamic model for the laser-membrane interaction. Furthermore, it allows us to use I as a measure of Σ. We then used the R_0 dependence of Σ_c to calibrate the value of I_c for tubes of different radii. This gave us a measure of $\epsilon = (I - I_c)/I_c = (\Sigma - \Sigma_c)/\Sigma_c$.

Propagation.—Figure 1 shows a typical propagating front. In these early stages the signal is close to the limit of optical resolution and barely perceptible above the thermal fluctuations. The instability becomes apparent once its amplitude exceeds a threshold value $u(z, t) = e^C$, where C is an amplification factor set by the experimental detection threshold. We found that the best way to identify and follow this leading edge of the propagating front was inspection by eye. This naturally adds some noise to the data. Below threshold, and even at zero tension, thermal fluctuations around the critical wavelength are strongly enhanced and obscure the instability as it initiates (see discussion below). Our measurements are also limited by the field of view of the camera. As seen in Fig. 1, this covers only about ten wavelengths on each side of the trap. As a result, we are insensitive to effects involving changes in velocity over larger distances. Once the initial front has passed we often saw an increase of the amplitude until it reaches a fully saturated nonlinear state. This larger amplitude, shorter wavelength state is still very different from the pearls discussed in [13].

From the fit of $X(t) = V(t - \Delta t)$, with $t = 0$ the time the laser was turned on, we extracted the front velocity V. Figure 2 shows a plot of the velocity as a function of ϵ. The velocity is scaled by the natural velocity scale in the membrane $V_\kappa = \kappa/\eta R_0^2$ where $\eta = 0.01$ P is the viscosity of water. Within the experimental accuracy the velocity scales linearly with a prefactor 0.04 ± 0.01, where the error is statistical. In comparison, GNPS predicted this linear relation with a prefactor of 0.09 (in our units). Taking into account that measured values for κ vary by factors of order unity, depending on the measurement technique, the agreement with GNPS is quite good. Measuring the front velocity is nontrivial even numerically: GNPS measured a velocity which was 25% lower than the analytical (MSC) estimate, while better resolution and improved front identification gave a result very close to the MSC prediction [15].

Wavelength selection.—The propagating front is characterized by a well defined wavelength which can be extracted from pictures such as those in Fig. 1. The dimensionless wave vector qR_0 is plotted in Fig. 3 as a function

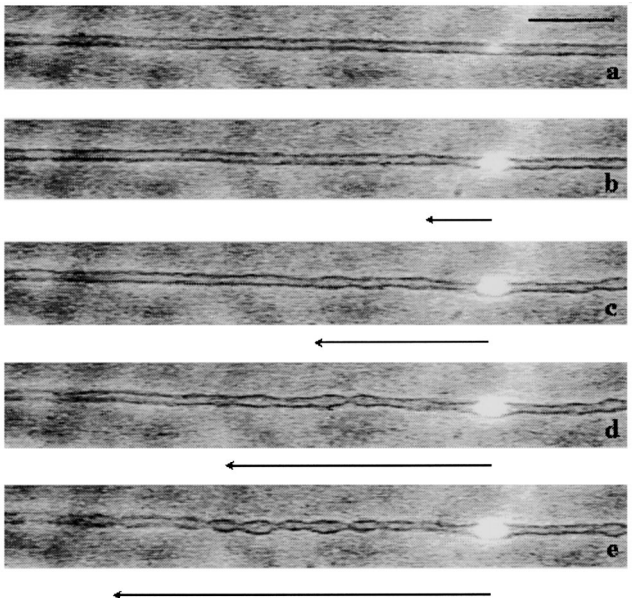

FIG. 1. Propagation of a pearling front outward from the illuminated laser spot for $\epsilon = 6.5$. Time from laser on in seconds: (a) 0.14, (b) 0.68, (c) 0.86, (d) 1.04, (e) 1.22. The bar represents 10 μm. The arrow gives our determination of the leading edge.

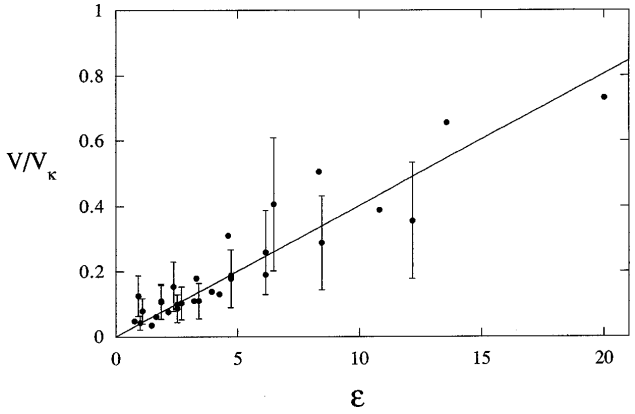

FIG. 2. Velocity of front propagation V scaled by $V_\kappa = \kappa/\eta R_0^2$ as a function of control parameter $\epsilon \equiv (I - I_c)/I_c = (\Sigma - \Sigma_c)/\Sigma_c$. A linear fit (solid curve) give 0.04 ± 0.01 for the slope.

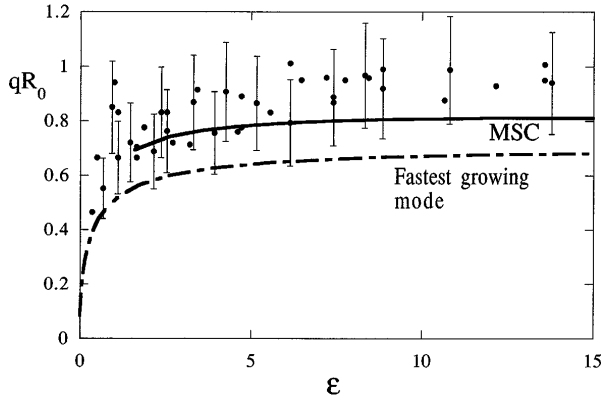

FIG. 3. Selected wave vector qR_0 as a function of ϵ. The theoretical prediction for fastest growing mode from the dispersion relation of GNPS (dashed curve) and their MSC wave vector correction [10,14] (solid curve) are also plotted.

of ϵ along with two theoretical results, the fastest growing mode of the linearized dispersion relation and the selected wave vector of the MSC. It is evident that the data correspond to smaller wavelengths than those predicted by the linear theory. There is much better agreement with the MSC prediction, especially for the moderate tension regime ($\epsilon \leq 5$). We believe that it is nonlinear effects that tend to shift the data at high tension values towards shorter wavelengths $qR \approx 1$.

A salient feature of the mean field theory that has evolved to describe this transition is that pearling occurs via a continuous bifurcation where the selected (or fastest growing) wave vector at threshold is zero and increases continuously with ϵ. We found experimentally that close to threshold pearling cannot propagate out and only develops a steady state "bulge" about 10 radii long centered around the laser position; see Figs. 4(a) and 4(b). This bulge is a localized, steady state for as long as the laser is kept on. It may hint at the existence of additional physical mechanisms such as steady state tension gradients in the tube [7,13,16], pressure gradients due to fluid entrainment [17], or stabilizing nonlinear effects.

At slightly higher ϵ we could indeed verify that long wavelengths tend to appear at onset [shown in Fig. 4(c)]. However, we could not measure the ϵ dependence, both because the signal is on the same level as the thermal fluctuations of the membrane and because these states are unstable, quickly supplanted by a shorter wavelength nonlinear state.

Measured "delay time."—From the fit $X(t) = V(t - \Delta t)$ in Fig. 2, the delay time Δt from $t = 0$ (power on) to the beginning of propagation can be measured as well. Figure 5 shows a log-log plot of the delay time Δt, scaled by the natural time scale $\tau_\kappa = R^3\eta/\kappa$, as a function of ϵ. Right near threshold, where a central bulge appears with no propagation, Δt was taken as the time it took for the bulge to develop. A clear trend is observed, and the best fit yields $\Delta t/\tau_\kappa = (1000 \pm 200) \times \epsilon^{-1.0\pm0.15}$. To check that the delay time scales with ϵ we fitted our data to $\Delta t \sim 1/\Sigma^\nu$ and obtained a worse fit (with $\nu = 1.4 \pm 0.2$).

Linear response theory.—Despite the nonlinear nature of the pearling, the leading edge of the instability has a moderate amplitude and hence can be analyzed in terms of the linear response [8,10,11]. We show here that the velocity calculation by GNPS using the MSC is in fact equivalent to the linear calculation by Gurin *et al.* [8], when extended to small values of ϵ. From this we shall further obtain an estimate for the delay time at the experimentally relevant regime of higher ϵ. We consider an approximate form of the exact dispersion relation of GNPS:

$$\omega(k) = \tau_\kappa^{-1} b k^2 \left[\frac{3}{2}\epsilon(1 - k^2) - k^2 - k^4 \right], \quad (1)$$

where $k = qR_0$ and $b \approx 0.04$. The initial perturbation, which is localized around the laser trap, is modeled by $u(z, t = 0) \sim \delta(z)$. The perturbation therefore diffuses from the origin and is amplified by the unstable modes

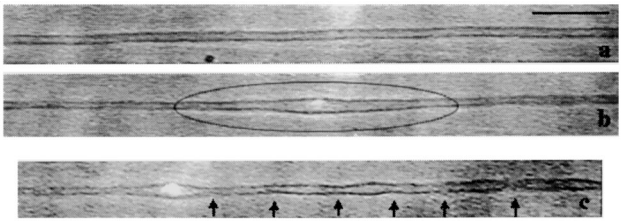

FIG. 4. Slightly above threshold long wavelengths appear as a steady state "bulge" centered around the position of the laser trap. Here (a) is the unperturbed tube and (b) is after 43 seconds of tweezing. In (c) we show a different tube with a long wavelength $qR_0 = 0.47$ close to threshold $\epsilon = 0.35$, corresponding to the lowest data point in Fig. 3. The arrows in (c) mark the troughs of the peristaltic mode, and the bright spot towards the left hand side of the frame marks the place of operation of the tweezers. The bar represents 10 μm.

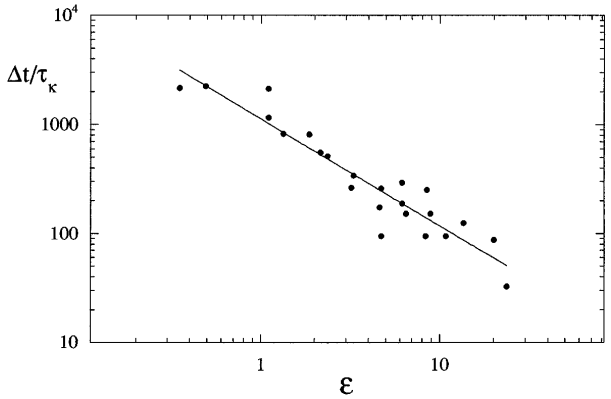

FIG. 5. Delay time Δt scaled by $\tau = R^3\eta/\kappa$ as a function of ϵ. The best fit (solid line) yields $\Delta t/\tau = (1000 \pm 200) \times \epsilon^{-1.0\pm0.15}$.

according to [8]

$$u(z,t) \sim \frac{1}{\sqrt{t}}\exp\left(-\frac{\Delta^2 z^2}{4R_0^2\omega_0 t}\right)\exp\left(ik_0\frac{z}{R_0} + \omega_0 t\right), \quad (2)$$

where we used a saddle point approximation with k_0 and ω_0 the wave number and the growth rate of the fastest growing mode, respectively, and $\Delta = [-2\omega_0/\omega''(k_0)]^{1/2}$. The leading edge follows the trajectory of constant amplitude $u(z,t) = e^C$:

$$z = 2\frac{\omega_0}{\Delta}t\sqrt{1 - \frac{C}{\omega_0 t}} \approx 2\frac{\omega_0}{\Delta}\left(t - \frac{C}{2\omega_0}\right). \quad (3)$$

Propagation is seen to begin after a delay time $\Delta t = C/2\omega_0$. Asymptotically, the front propagates at a constant velocity $V/V_\kappa = 2\omega_0/\Delta$. Inserting the theoretical values for k_0, ω_0, we see that close to threshold, $\epsilon \ll 1$, the critical scaling is [8] $V/V_\kappa = 0.2\epsilon^{3/2}$ and $\Delta t/\tau_\kappa = 21C\epsilon^{-2}$. However, for the experimental regime, $\epsilon \geq 1$ the critical scaling crosses over to

$$\frac{V}{V_\kappa} = 0.09\epsilon; \qquad \frac{\Delta t}{\tau_\kappa} = 33C\epsilon^{-1}. \quad (4)$$

The result for V is identical to the GNPS result. The factor C in Δt characterizes the amplification needed to get an observable instability amplitude from the initial perturbation. While the measured delay time is thus consistent with linear response, we cannot rule out the possibility that it is related to a mechanism for production of tension in the membrane [7,16]. Furthermore, the experimental value $C \approx 30$ is higher by a factor of 3–5 than one would reasonably estimate, mainly due to the high amplitude needed to detect the leading edge.

Role of fluctuations.—Experimentally, the analysis of the propagating front was complicated by the existence of fluctuations in the tube which, at times, were on the order of the instability itself. This is made worse by the proximity of the wavelength at which the thermal fluctuations below onset peak to the unstable mode of the instability itself. Equipartition in the case of curvature with no tension gives the amplitude u_k of the mode with wave number $k = qR_0$ in a fluctuating cylinder at equilibrium: $\langle|u_k|^2\rangle \propto \frac{k_BT}{\kappa}(\frac{3}{2} - \frac{1}{2}k^2 + k^4)^{-1}$. This has a maximum at $k = \frac{1}{2}$, close to the wavelengths observed at threshold. Plugging in all factors and integrating gives the root mean squared fluctuation to be about $0.1R_0$, which is consistent with what we see below onset. Intriguing questions, and ones that we cannot answer at present, are how the masking of the linear regime occurs, and what is the mechanism by which the fluctuations interact with the instability.

In summary, we have quantitatively examined pattern formation in the pearling instability of fluid membrane tubes. At onset thermal perturbations mask and compete with the low amplitude, linear instability. The observations of propagating fronts allow us to compare measurements of velocity, delay time, and wavelength in the nonlinear state with linear theory at the leading edge. Predictions that rely on gradients between the trap and globule at the edge of the tube, for example slowing of the front at large distances [7,16], are beyond the scope of our measurements. We find that the measurements are qualitatively consistent with a continuous bifurcation with long wavelength at threshold, though in the immediate vicinity of the transition this behavior is masked by thermal fluctuations. Above threshold, quantitative measurements of the front velocity, delay time, and wavelength compare well with our linear analysis and the recent theoretical predictions by GNPS.

We thank R. Goldstein, R. Granek, V. Lebedev, F. MacKintosh, P. Nelson, Z. Olami, T. Powers, S. Safran, and U. Seifert for fruitful discussions, and J.-P. Eckmann for raising the question of propagation. Work supported by the BSF Grant No. 94–00190, the Klutznick Foundation, the Minerva Center for Nonlinear Physics, and the Minerva Foundation, Munich.

[1] W. Helfrich, Z. Naturforsch. **28c**, 693 (1973).
[2] R. Lipowsky, Nature (London) **349**, 475 (1991); X. Michalet, F. Julicher, B. Fourcade, U. Seifert, and D. Bensimon, La recherche No. 269, Vol. 25 (1994).
[3] W. Helfrich and R.-M. Servuss, Nuovo Cimento **3**, 137 (1984).
[4] E. Evans and W. Rawicz, Phys. Rev. Lett. **64**, 2094 (1990).
[5] R. Bar-Ziv and E. Moses, Phys. Rev. Lett. **73**, 1392 (1994).
[6] P. Nelson. T. Powers, and U. Seifert, Phys. Rev. Lett. **74**, 3384 (1995).
[7] R. Granek and Z. Olami, J. Phys. II (France) **5**, 1349 (1995).
[8] K. L. Gurin, V. V. Lebedev, and A. R. Muratov, JETP **83**, 321 (1996).
[9] A. Ashkin, Phys. Rev. Lett. **24**, 156 (1970); Science **210**, 1081 (1980).
[10] R. E. Goldstein, P. Nelson, T. Powers, and U. Seifert, J. Phys. II (France) **6**, 767 (1996).
[11] G. Dee and J. S. Langer, Phys. Rev. Lett. **50**, 383 (1983); G. Ahlers and D. Cannell, Phys. Rev. Lett. **50**, 1583 (1983); J. Fineberg and V. Steinberg, Phys. Rev. Lett. **58**, 1332 (1987); W. van Saarloos, Phys. Rev. A **37**, 211 (1988).
[12] K. Svoboda and S. M. Block, Annu. Rev. Biophys. Biomol. Struct. **23**, 247 (1994).
[13] J. L. Goveas, S. T. Milner, and W. B. Russel, J. Phys. II (France) (to be published).
[14] T. Powers (private communication).
[15] T. Powers and R. Goldstein, Phys. Rev. Lett. **78**, 2555 (1997).
[16] P. D. Olmsted and F. C. MacKintosh, J. Phys. II (France) **7**, 139 (1997).
[17] P. Nelson (private communication).